Available online at www.sciencedirect.com
SCIENCE DIRECT®
PERGAMON
Acta Astronautica 56 (2005) 547–553
ACTA ASTRONAUTICA
www.elsevier.com/locate/actaastro

# Korea's first satellite for satellite laser ranging

Jun Ho Lee[a,*], Seung Bum Kim[a], Kyung Hee Kim[a], Sang Hyun Lee[a], Yong Jo Im[a], Yang Fumin[b], Chen Wanzhen[b]

[a] *Satellite Technology Research Center, Korea Advanced Institute of Science & Technology (KAIST), 373-1 Guseong-dong, Yusong-gu, Daejeon, 305-701, Republic of Korea*
[b] *Shanghai Observatory, Chinese Academy of Sciences, 80 Nandan Rd., Shanghai 200030, China*

Received 11 December 2003; received in revised form 15 February 2004; accepted 13 September 2004
Available online 13 December 2004

**Abstract**

Science Technology Satellite-2 (STSAT-2) has been developed since October 2002 as a sequel mission to KAISTSAT-4 (STSAT-1). STSAT-2 is scheduled to be launched into an ellipsoidal orbit of 300 km × 1500 km in December 2005 by the first Korea Satellite Launch Vehicle KSLV-1. STSAT-2 has two payloads: a Lyman-α imaging solar telescope and a laser reflector array (LRA) for satellite laser ranging. The paper first presents a brief introduction to the STSAT-2 program. Preliminary designs of the LRA payload and STSAT-2 are provided with anticipated performance results followed by an analysis of safety issues related to the electro-optical devices on STSAT-2.


## 1. Introduction

The Satellite Technology Research Center (SaTReC) in the Korea Advanced Institute of Science and Technology (KAIST) has developed and operated Korea's first two satellites (KITSAT-1, 2), and the nation's first earth observation satellite (KITSAT-3) and space science satellite (KAISTSAT-4 or STSAT-1) [1–5]. The Center is currently developing Science Technology Satellite-2 (STSAT-2) [6], which is the second satellite of the STSAT series designated in the long-term plan for Korea's space development (Fig. 1) by the Ministry of Science and Technology of Korea in 2000.

STSAT-2 is a micro-satellite of ∼ 90 kg for satellite technology research and space science. The engineering objective of STSAT-2 is to provide a test-bed for satellite core technology including a fine digital sun sensor and a double-head star tracker, while the primary scientific objective of STSAT-2 is to provide solar imaging at Lyman-α (0.121 μm).

STSAT-2 will be launched into an ellipsoidal orbit of 300 km × 1500 km with an inclination angle of 80°. As such, with satellite laser ranging (SLR), it will provide a unique opportunity to investigate in a precise manner the variations of an ellipsoidal orbit. Additionally, the precise orbit determination will be used to evaluate the performance of the first Korean

* Corresponding author. Tel.: +82 42 869 8643; fax: +82 42 861 0064.
*E-mail address:* jhl@satrec.kaist.ac.kr (J.H. Lee).

0094-5765/$ - see front matter © 2004 Elsevier Ltd. All rights reserved.
doi:10.1016/j.actaastro.2004.09.048

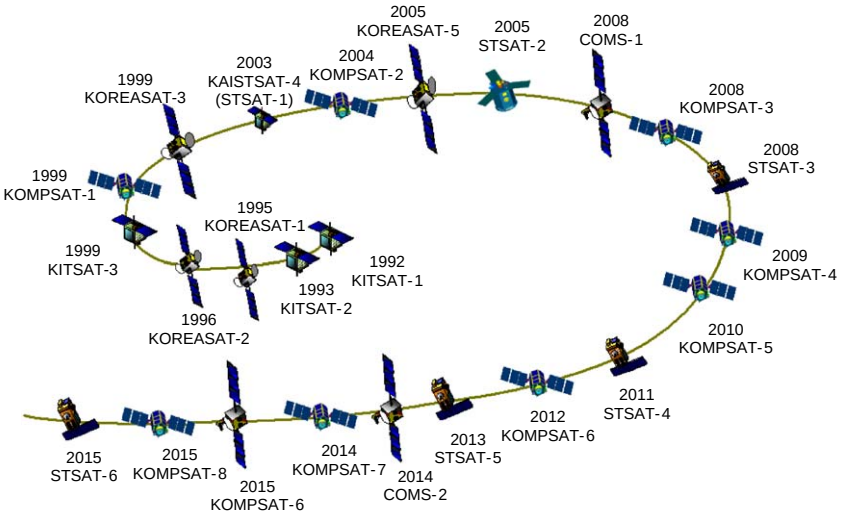


Fig. 1. Long-term plan for korea's space development.

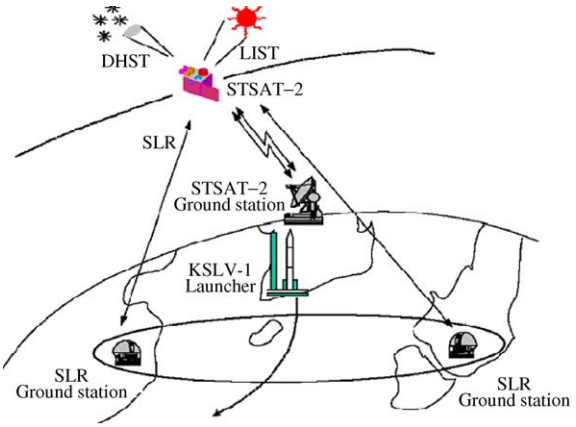


Fig. 2. Operation of STSAT-2.

satellite launcher. Fig. 2 shows operational concepts of STSAT-2. A ground station of STSAT-2 will be located at SaTReC, while STSAT-2 will be tracked by SLR ground stations including the Shanghai Observatory in China and the NERC space geodesy facility in the UK.

This paper presents a preliminary design of a payload for satellite ranging of STSAT-2. The expected performances are then analyzed followed by an outline of the safety issues of electro-optic sensors of STSAT-2.

## 2. Preliminary design of STSAT-2 with laser reflector array (LRA)

### *2.1. Preliminary design of LRA*

The LRA is a simple passive payload instrument consisting of 9 prisms. Each prism or corner cube is a 30 mm (clear aperture) cylinder of fused silica containing a three-surface corner mirror. The corner cubes are symmetrically mounted on a hemispherical surface with a nadir-looking corner cube in the center, surrounded by an angled (40°) ring of eight corner cubes. The diameter of the assembly is 200 mm. Each corner cube has a divergence of $12 \pm 2''$ in order to take into account satellite velocity aberrations. Fig. 3 shows 3D modeling of LRA.

The prisms reflect short laser pulses back to the transmitting ground station in a field of view angle of 360° in azimuth and 60° in elevation around the perpendicular to the centered corner cube.

### *2.2. Preliminary design of STSAT-2 with LRA*

STSAT-2 is a micro-satellite of $\sim$ 90 kg with two payloads: a Lyman-$\alpha$ imaging solar telescope (LIST), which was separately developed by Kyung Hee University of Korea, and an LRA. The platform of STSAT-2 is designed so as to provide test-beds for core tech-

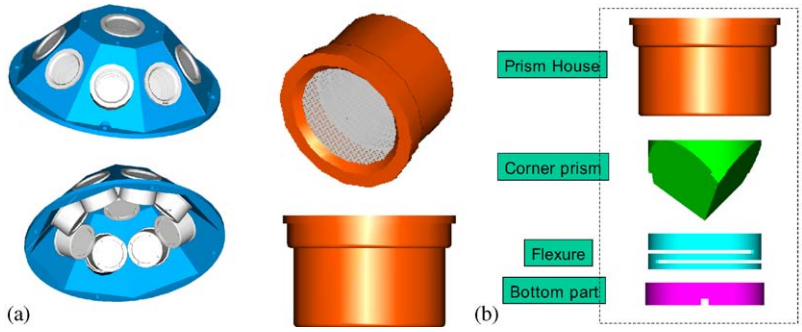


Fig. 3. 3D modeling of LRA: (a) LRA, (b) Single retro-reflector assembly.

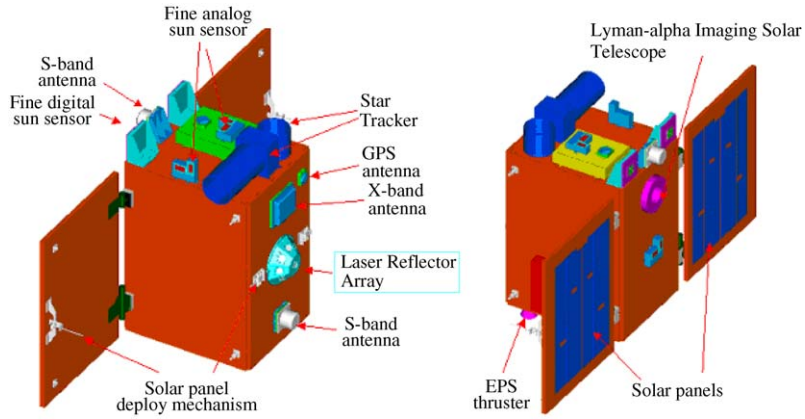


Fig. 4. Primary Design of STSAT-2.

nology experiments and to satisfy payload requirements. At the time of this writing, the modular structure of STSAT-2 has been preliminarily designed and is currently in the optimization process. Fig. 4 shows the preliminary design of STSAT-2 and Table 1 summarizes the specifications of STSAT-2.

## 3. Performance predictions

### 3.1. Effective area calculation

The effective area of an LRA can be driven as a function of azimuth and elevation angles of incoming laser, as illustrated in Fig. 5:

$$A_{total}(\theta_e, \theta_a) = \sum_{i=0}^{N=8} A_i(\theta_i(\theta_e, \theta_a)), \quad (1)$$

Table 1
Specifications of STSAT-2

| Item | Specification |
|---|---|
| Sponsor | Ministry of Science and Technology of Korea |
| Expected life | 2 years |
| Primary application | Satellite engineering experiments<br>Solar imaging at Lyman-$\alpha$ (0.121 μm) |
| Primary SLR Application | Precise orbit determination |
| Launch date (planned) | Dec. 2005 (by KSLV-1) |
| Orbit | Elliptical |
| Inclination | 80° |
| Perigee | 300 km |
| Eccentricity | 0.082435 |
| Period | 102.998 min |
| Attitude control | 3-axis stabilization, 0.15° pointing accuracy |
| Weight | 90 kg (Platform + Payloads) |

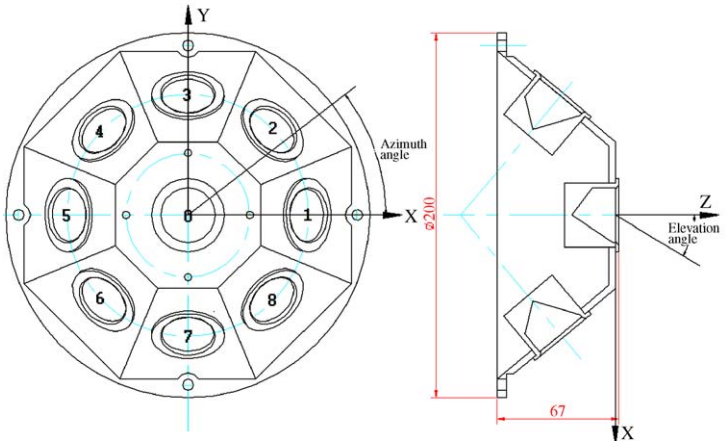


Fig. 5. Definition of numbering of retro-reflectors, and azimuth and elevation angles.

where $A_{total}$ = the total effective area of the LRA, $A_i$ = the effective area of the $i$th retro-reflector, $\theta_a$ = azimuth angle, $\theta_e$ = elevation angle, $\theta_i$ = angle of incidence of the laser beam to the $i$th retro-reflector, and $N$ = the total number of surrounded corner cubes.

The effective area of the $i$th single retro-reflector $A_i$ in Eq. (1) can be written as follows:

$$A_i(\theta_e, \theta_a) = \pi r^2 \frac{(\sin^{-1}\mu - \sqrt{2}\mu\tan\theta_i')\cos\theta_i}{2}, \quad [7] \tag{2}$$

$$\theta_i(\theta_e, \theta_a) = \cos^{-1}\left(\frac{1}{2}\frac{\vec{a}_i\cdot\vec{R} + |\vec{a}_i\cdot\vec{R}|}{|\vec{a}_i||\vec{R}|}\right), \tag{3}$$

$$\theta_i' = \sin^{-1}\left(\frac{\sin\theta_i}{n}\right), \tag{4}$$

$$\mu = \sqrt{1 - 2\tan^2\theta_i'} \tag{5}$$

$$\vec{R} = \begin{cases} \vec{k} & \text{if } \theta_e = 0, \\ \cos\theta_a\vec{i} + \sin\theta_a\vec{j} + \cot\theta_e\vec{k} & \text{otherwise,} \end{cases} \tag{6}$$

$$\vec{a}_i = \begin{cases} \vec{k} & \text{if } i = 0, \\ \sin\theta_t\cdot\cos\left(\frac{360^\circ}{N}(i-1)\right)\vec{i} & \\ +\sin\theta_t\cdot\sin\left(\frac{360^\circ}{N}(i-1)\right)\vec{j} & \\ +\cos\theta_t\vec{k} & \text{otherwise,} \end{cases} \tag{7}$$

where $r$ = the radius of a single retro-reflector, $n$ = the refractive index of a single retro-reflector, $\theta_i'$ = the refracted angle of incidence, $\vec{a}_i$ = the directional vector of the $i$th retro-reflector prism front surface, $\vec{R}$= the directional vector of an incoming laser, and $\theta_i$ = the slope angle of angled eight corner cubes (in our design, 50°).

Fig. 6 shows the normalized effective areas of a single retro-reflector to the incidence angle and of the LRA to the elevation angles. The area of the single retro-reflector's clear aperture normalizes both the effective areas. The effective area of LRA is larger than the front surface area of a single corner cube over a field of view angle of 360° in azimuth and 60°in elevation.

### 3.2. Calculation of photoelectron numbers

Calculation of photoelectron numbers $n$ was performed according to the following equation:

$$n \approx \frac{1}{SF}\frac{E_{tr}}{h\nu}K_T K_{LRA} K_R \frac{D_{LRA}^2 D_R^2 T^2}{H^4\theta_l^2\theta_{LRA}^2}\eta, \tag{8}$$

where $E_{tr}$= Transmitted energy, (30 mJ)

$E_{ph} = h\nu$ : Photon energy at working wavelength, $E_{ph} = h\nu = 3.74\times10^{-19}$ J

$K_T$= Transmission coefficient of optical transmitting telescope (0.7)

$T$= Atmospheric transmission coefficient in zenith (0.5)

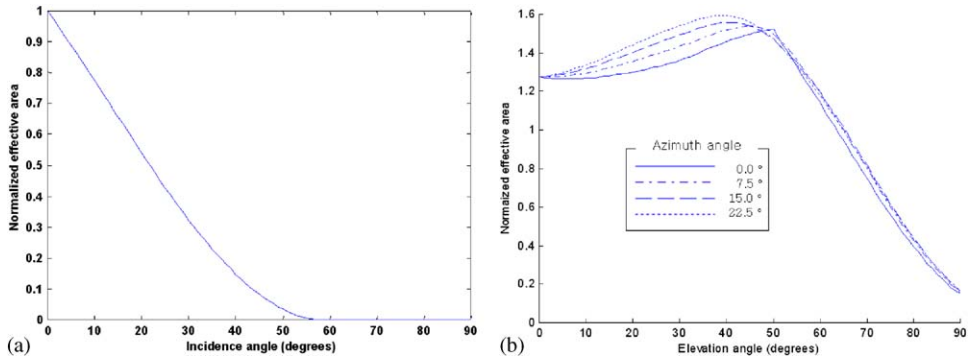


Fig. 6. Normalized effective areas of (a) single retro-reflector, and (b) LRA.

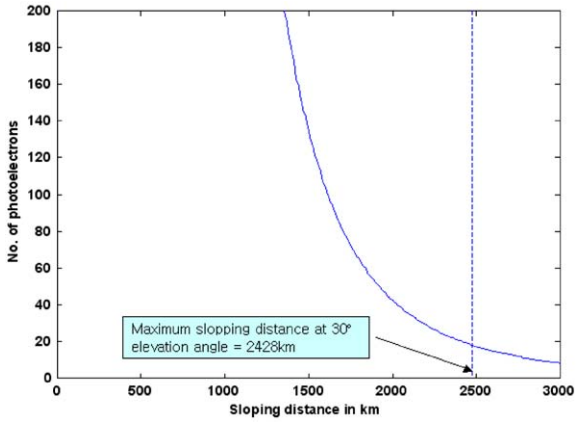


Fig. 7. Number of photoelectrons.

$\theta_l$= Divergence of laser beam (30″)

$\theta_{LRA}$= Divergence of RR (LRA) (15″)

$H$= Sloping distance from the ranger to the RR

$D_{LRA}$= Effective diameter of the RR (> 30 mm)

$K_{LRA}$= Transmission coefficient of corner cubes including reflective losses (0.6)

$D_R$= Diameter of receiving aperture (60 cm)

$K_R$= Transmission coefficient of receiving telescope (0.7)

$\eta$= Quantum efficiency of photon receiver (20%)

$SF$= Safety factor (5).

The numbers are for the SLR ground station at the Shanghai Observatory of China [8]. Fig. 7 plots the number of the detected photons at the Shanghai Observatory of China against the sloping distance. The detected photons are approximately 20 even at the longest sloping distance, and thus the STSAT-2 can be tracked over its entire orbit.

Table 2
Geological information of Shanghai Observatory and NERC space geodesy facility

| SLR station | Latitude | Longitude | Altitude |
|---|---|---|---|
| Shanghai Observatory | 31.097540 | 121.191737 | 74.404 m |
| NERC space geodesy facility | 50.8611380 | 0.336122 | 27.832 m |

### 3.3. Contact time analysis

The contact time between SLR ground stations and STSAT-2 was calculated using commercial software [9]. The analysis was conducted for two SLR stations, the Shanghai Astronomical Observatory in China and the NERC space geodesy facility in the UK, which agreed to track STSAT-2 at the time of this writing.

The analysis assumes that STSAT-2 will be launched on December 31st 2005 and SLR tracking is possible when the elevation angle between the SLR ground stations and STSAT-2 is greater than 30°. Table 2 lists geological information of the Shanghai Observatory and the NERC space geodesy facility. Table 3 summarizes the total number of contacts for SLR with average time of contacts. The Shanghai Observatory was assumed to track the STSAT-2 only during night, while the NERC space geodesy facility tracks throughout the day. Fig. 8 shows the variation of contact time for 30 days from the first day of January 2005. Shanghai Observatory has 185 contacts with 4.85 min contact time while NERC has 483 contacts with 5.74 min contact time.

Since LIST is the primary payload of STSAT-2, STSAT-2 will normally operate with sun-pointing atti-

Table 3
Contact time analysis results

| SLR station | Number of contacts for the first year after launch | | | |
|---|---|---|---|---|
| | Total | When duration is longer than 1 min | Observable | Average contact time (min) per contact |
| Shanghai | 675 | 601 | 189 (night only) | 4.85 |
| NERC | 533 | 483 | 483 | 5.74 |

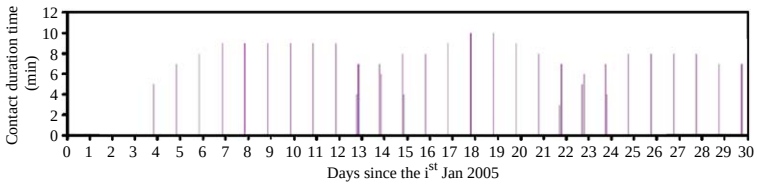


Fig. 8. The contact time variation for the 30 days from the 1st January 2005.

Table 4
Laser energy density calculation deposited on electro-optical devices of STSAT-2

| Sensor | Operating wavelength | Attenuation at 532 nm | Pixel size (μm) | Aperture size | Deposited energy (nJ) | Deposited energy density (mJ/cm$^2$) |
|---|---|---|---|---|---|---|
| LIST | 0.121 μm | 0.05 | 24 | 76.2 mm | 30 | 5.2 |
| DHST | Visible | 0.95 | 13 | 50 mm | 62 | 37 |
| DSS | 0.88 μm | 1e−5 | 25 | Pin-hole | 2.6 | 0.4 |

tude control except during periods of communication with the ground system located at Daejeon, South Korea. SLR stations located in Asian countries will almost always have a line of sight to the LRA on STSAT-2, which is located on the same plane with the X-band and S-band communication antennas, while SLR stations outside Asian countries have limited lines of sight to the LRA depending on the operational scenarios of STSAT-2.

## 4. Safety issues of electro-optical devices of STSAT-2

Safety concerns of electro-optical devices (CCDs) of STSAT-2 have been addressed from the beginning of STSAT-2 development. Similar safety issues are raised in the UoSAT microsatellite program [10]. STSAT-2 has three electro-optical devices: a Lyman-α Solar Imaging Telescope (LIST), a Double-Head Star Tracker (DHST) and a Digital Sun Sensor (DSS) (Refer Fig. 4).

The SLR laser energy density deposited on the detectors is calculated with the information of Shanghai Observation SLR station [8], and summarized in Table 4. The results show that energy densities deposited on all the devices are 1000 times less than the CCD breakdown voltage (0.3 J/cm$^2$) [11].

## 5. Conclusions

This paper presents the preliminary designs of LRA and STSAT-2 followed by a brief introduction of STSAT-2. The analysis shows that the effective area of the LRA is greater than 707 mm$^2$ over a field of view angle of 360°in azimuth and 60°in elevation. The Shanghai SLR ground station can detect more

than 20 photons returned by the LRA of STSAT-2 over its entire elliptical orbit of 300 km × 1500 km. Finally, all electro-optical devices of STSAT-2 are found to be safe from SLR lasers.

## Acknowledgements

We would like to express our appreciation to the Shanghai Observatory of China and the NERC Space Geodesy in the UK for their generous assistance and offer to track STSAT-2 in the future.

## References

[1] Soon-Dal Choi, Byung Jin Kim, Ee-Eel Kim, an introduction to the KITSAT program and the activities at the SaTReC in Korea, Soon-Dal Choi, Proceedings of the Cospar Colloquium on Scientific Microsatellite, 1997.
[2] Sungdong Park, Dan Keun Sung, Soon Dal Choi, Overview of KITSAT-1/2 microsatellite systems, Journal Astronamy and Space Science 13 (20) (1996) 1–19.
[3] Young-Hoon Shin, Sun-Mee Park, Kyoung-Wook Min, Sung-Heon Kim, Space Radiation Effect monitored by KITSAT-1 and KITSAT-2, Proceedings of the 9th Annual AIAA/USU Conference on Small Satellites, 1999.
[4] B.J. Kim, H. Lee, S.D. Choi, Three-axis reaction wheel attitude control system for KITSAT-3 microsatellite, Space Technology, vol. 16, Pergamon, New York, 1997, pp. 191–296.
[5] Sungdong Park, Taejin Chung, Hyunwoo Lee, Yunhwang Jeong, Jingjoong Kim, Younghoon Shin, Dae Keun Sung, Soon Dal Choi, KITSAT-3 launch and operation, Small Satellite Symposium, Japan, 1999.
[6] Jong Tae Lim, Myeong-Ryopng Nam, Kwang-Sun Ryu, Kyung-Mo Tahk, Sung-Ho Lee, Kyung-Hee Kim, Exploring space on a small satellite, STSAT-2: a test bed for new technologies, 14th Annual AIAA/USU Conference on Small Satellites, 2003.
[7] Peter O. Minott, Design of retrodirector arrays for laser ranging of satellites, NASA-TM-X-70657, 1974.
[8] Yang Fumin, Current status and future plans for the Chinese satellite laser ranging network, Surveys in Geophysics 22 (2001) 465–471.
[9] “Satellite Tool Kit”, Analytical Graphics, Inc.
[10] M. Unwin, A study into the use of laser retroreflectors on a small satellite, International Journal of Small Satellite Engineering 1 (1) (1995).
[11] C. Zhang, T. Benchetrit, S. Watkins, R. Walser, M. Becker, Laser-Induced Damage to Photosensor Arrays, Proceedings of 22nd Annual Boulder Damage Symposium, 1989.